

# Tailormade: $K_3\{Li[IrO_4]\} = K_6^1[(O_{2/2}LiO_2IrO_{2/2})_2]$ , the first lithooxoironate\*

Klaus Mader and Rudolf Hoppe\*\*

Institut für Anorganische und Analytische Chemie I der Justus-Liebig-Universität, Heinrich-Buff-Ring 58, D-35392 Giessen (Germany)

(Received November 13, 1993)

## Abstract

We obtained previously unknown  $K_3\{Li[IrO_4]\}$  in the form of dark-red elongated single crystals, by heating well-ground mixtures of  $Li_2IrO_3$  and  $KO_{0.51}$  (molar proportions Ir:K, 1.00:3.76) in an “Ag cylinder” (at 1073 K for 71 days).  $K_3\{Li[IrO_4]\}$  crystallizes as mC36 in the space group  $C2/c$ , with  $a = 1067.29(9)$  pm,  $b = 986.36(8)$  pm,  $c = 587.70(5)$  pm and  $\beta = 103.938(8)^\circ$ ;  $Z = 4$ . Refinement of the structure with 949 reflections ( $F_o > 3\sigma(F_o)$ ) from 1032 independent reflections (merged from 4137  $I_o(hkl)$ ) gave  $R = 0.0351$  and  $R_w = 0.0378$ . The structure is characterized by Vierer single chains  ${}^\infty[(O_{2/2}LiO_2IrO_{2/2})_2]$  isolated from one another. Their arrangement corresponds to the configuration of a densest packing of “tree-trunks”. The effective coordination numbers, mean fictive ionic radii and the Madelung part of the lattice energy, as well as the charge distribution are calculated and discussed.

## 1. Introduction

During the past few decades, a huge number of polynary metal oxides of the alkaline metals have been prepared and structurally characterized. Despite the diversity of crystal structures, we found that, in contrast to Cs, Rb and K, Li often acts as an ordering medium.

In the case of oxides  $A_3\{MO_4\}$  ( $A \equiv K, Rb, Cs; M \equiv V, Mn$ ) [1], the crystal structures could not be solved completely, because of the statistical orientation of the pseudo-sphere-like anions  $[MO_4]$ . However, compared with that, derivatives  $A_{3-x}Li_x\{MO_4\}$ , such as  $K_2\{Li[VO_4]\}$  [2] and  $K_{11}\{Li[MnO_4]_4\}$  [3], show complete ordering. The first example is characterized by layers  $\{Li[VO_4]\}$ , while neo-pentane-like groupings  $\{Li[MnO_4]_4\}$  dominate the structure in the manganate(V).

Within the sequence  $Li_4[IrO_4] \cdots Cs_4[IrO_4]$  [4–7], the first member is still missing. Therefore, the leading question of this investigation concerns whether or not it is possible to create quaternary oxides similar to  $K_3Li[IrO_4]$  and, if so, will it be a “lithoironate(IV)” with chains or rings as independent units built by coordination polyhedra of Ir and Li. A side view on oxosilicates indicates that in  $K_3\{Li[SiO_4]\}$  [8] chains  $\{Li[SiO_4]\}$  occur as a main feature of the crystal structure.

## 2. Experimental details

### 2.1. Preparation and properties of $K_3\{Li[IrO_4]\}$

The starting materials were as follows:  $KO_{0.51}$ , obtained by controlled oxidation of potassium (Riedel de Haën, 98%, purified by liquation) with dry oxygen [9];  $Li_2IrO_3$ , obtained by heating intimate mixtures of  $Li_2O$  and  $IrO_2$  (Li:Ir = 2.20:1.00) in an “Ag-cylinder” for 30 days at 973 K.

$Li_2O$  was prepared via dehydration of  $LiOH \cdot H_2O$  (Riedel de Haën, 97%) [10]. Active  $IrO_2$  was obtained by oxidation of  $IrCl_3$  (Degussa, 64.3% Ir) with dry oxygen at 833 K. Under an argon atmosphere, intimate mixtures of  $Li_2IrO_3$  and  $KO_{0.51}$  (Ir:K = 1.00:3.76) were prepared, then transferred into an “Ag-cylinder”, and finally sealed into a silica tube. Within 2 days, the temperature was raised to 673 K, after which it was slowly (within 7 days) increased to 1073 K. After annealing for 71 days, the samples were cooled to room temperature at rates of 50–70 K per day.

Thus, we obtained dark crystalline samples coloured brown after grinding. They contained single crystals of  $K_3\{Li[IrO_4]\}$  of good quality, which were mostly elongated in shape. Some small individuals obtained were magnificent dark red.

However, no formation of  $K_3\{Li[IrO_4]\}$  was observed in the powder pattern of samples prepared by heating intimate mixtures of the binary oxides  $IrO_2$ ,  $Li_2O$  and  $K_2O$  in appropriate molar proportions. Once again, “exchange reactions” [11] proved to be a valuable

\*This article represents part of the thesis of Klaus Mader.

\*\*Author to whom correspondence should be addressed.

TABLE 1. Crystal data and details of data collection and statistics for  $K_3\{Li[IrO_4]\}$ 

Pearson symbol	mC36
Spacegroup	$C2/c$ (no. 15 IT)
Lattice parameters (Guinier data)	$a = 1067.29(9)$ pm $b = 968.36(8)$ pm $c = 587.70(5)$ pm $\beta = 103.938(8)^\circ$
Density (X-ray)	$4.29 \text{ g cm}^{-3}$
Molar volume (X-ray)	$88.8 \text{ cm}^3 \text{ mol}^{-1}$
Molar volume (sum of binary oxides)	$86.9 \text{ cm}^3 \text{ mol}^{-1}$
Crystal shape, colour	Elongated, red
Linear absorption coefficient $\mu$	$235.78 \text{ cm}^{-1}$ (Mo $K\alpha$ )
Data collection	Siemens AED 2 diffractometer, Mo $K\alpha$ ( $\lambda = 71.069 \text{ \AA}$ ), graphite monochromator, $\omega$ scan, profile-fit, $3^\circ \leq \theta \leq 32^\circ$
Data correction	Lp-factors, absorption via "psi-scans"
Data statistics	4137 $I_o(hkl)$ measured, merged to 1032 independent reflections, 949 with $F > 3\sigma(F_o)$ used for refinement, $F(000) = 644$ ; 45 parameters refined
Structural refinement	SHELX-76 and SHELXS-86, Patterson map, difference maps, "full matrix least- squares" refinements, "anisotropic" thermal parameters, $R = 0.0351$ ; $R_w = 0.0378$ ; $w = 3.2742/(\sigma^2(F) + 0.000743F)$

TABLE 2. Positional ( $\times 10^4$ ) and thermal ( $\text{pm}^2$ ) parameters in  $C2/c$  for  $K_3\{Li[IrO_4]\}$ , with standard deviation in parentheses

Atom	Wyckoff position	x	y	z			
Ir	4c	2500	2500	0			
K(1)	8f	6542(1)	5893(1)	4746(2)			
K(2)	4e	0	4054(2)	2500			
Li	4e	0	7343(15)	2500			
O(1)	8f	4110(3)	6762(4)	4709(6)			
O(2)	8f	6584(4)	1372(4)	2459(7)			
		$U_{11}$	$U_{22}$	$U_{33}$	$U_{12}$	$U_{13}$	$U_{23}$
Ir		140(2)	112(2)	133(2)	-6(1)	52(1)	-2(1)
K(1)		244(5)	188(5)	202(5)	-1(4)	93(4)	-5(4)
K(2)		326(9)	208(7)	350(9)	0	136(7)	0
Li		193(86)	186(59)	200(84)	0	60(65)	0
O(1)		158(16)	230(16)	228(17)	40(14)	78(13)	-41(14)
O(2)		189(17)	203(17)	269(19)	-18(13)	30(14)	-96(14)

The "anisotropic" thermal factor has the following form:  
 $\exp -2\pi^2(U_{11}h^2a^{*2} + U_{22}k^2b^{*2} + U_{33}l^2c^{*2} + 2U_{23}k^2l^2b^*c^* + 2U_{13}h^2l^2a^*c^* + 2U_{12}h^2k^2a^*b^*)$

synthesis tool to obtain compounds that cannot be prepared in the traditional way by annealing binary oxides. The aqueous solution of  $K_3\{Li[IrO_4]\}$  is dark blue. In air, the oxide decomposes immediately. Consequently, single crystals had to be collected under with sodium wire dried paraffine.

TABLE 3. Motifs of mutual adjunction, ECoN and MeFIR for  $K_3\{Li[IrO_4]\}$  (distances and MeFIR in pm)

	$2O(1)^{2-}$	$2O(2)^{2-}$	CN	ECoN	MeFIR
$1Ir^{4+}$	2/1 190.6	2/1 191.7	4	4.0	51.1
$2K(1)^+$	1/1 + 1/1 + 1/1 267.8 270.3 272.4	1/1 + 1/1 + 1/1 267.3 308.6 315.1	6	5.2	134.9
$1K(2)^+$	2/1 284.7	2/1 + 2/1 281.4 302.5	6	5.9	148.3
$1Li^+$	2/1 189.6	2/1 194.0	4	4.0	51.4
CN	6	7			
ECoN	6.0	6.3			
MeFIR	138.3	142.4			

Starting values for ionic radii: standard  $R(O^{2-}) = 140$  pm; with weighted mean distances  $\bar{d}(\text{cation}-O^{2-})$  and following the ECoN concept, we obtained  $R(Ir^{4+}) = 51.07$  pm;  $R(K(1)^+) = 134.87$  pm;  $R(K(2)^+) = 148.20$  pm;  $R(Li^+) = 51.51$  pm.

Note the difference in MeFIR for K(1) and K(2).

## 2.2. X-ray investigations

A powdered sample was characterized at room temperature by a modified Guinier technique [12] with  $\alpha$ -quartz ( $P3_121$ ,  $a = 491.26$  pm and  $c = 540.23$  pm) as internal standard, using Cu  $K\alpha_1$  radiation ( $\lambda = 154.051$  pm). The diffraction pattern could be indexed according to a C-centered monoclinic unit cell:  $a =$

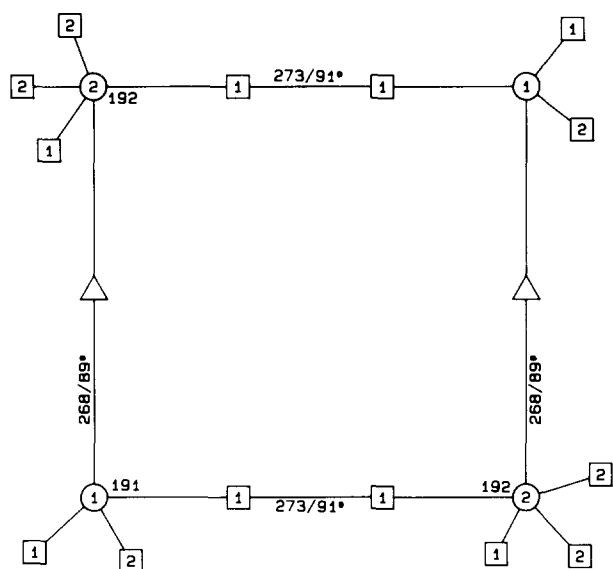


Fig. 1. Schlegel projection/diagram of CP(Ir) in  $K_3\{\text{Li}[\text{IrO}_4]\}$ , showing distances  $d(\text{Ir}-\text{O})$  and  $d(\text{O}-\text{O})$ , as well as angles  $\text{O}-\text{Ir}-\text{O}$ :  $\Delta$ , Li;  $\square$ , K;  $\circ$ , O.

1067.29(9) pm,  $b = 986.36(8)$  pm,  $c = 587.70(5)$  pm and  $\beta = 103.938(8)^\circ$ .

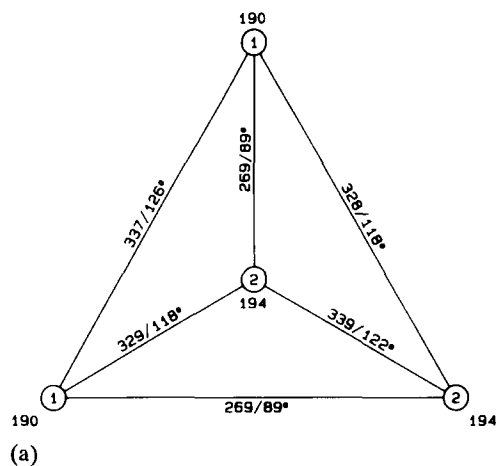
We collected a large number of crystals. After sealing them into Mark capillaries, they all were checked by X-ray examination. The crystal which was apparently the best was then used to make a rotation photograph (around [001]) and Weissenberg photographs ( $(hk0)$  and  $(hk1)$ ). These photographs confirmed the results of the Guinier examination. Only  $hkl$  reflections with  $h+k=2n$  were observed.

The single crystal was then mounted on a Siemens AED 2 diffractometer (Mo  $K\alpha$ ,  $\lambda = 71.069$  pm, graphite). We recorded 4137  $I_o(hkl)$  which finally merged to 1032 independent reflections. The absorption was corrected semi-empirically via "psi-scans". For details of the data collection and data statistics, see Table 1.

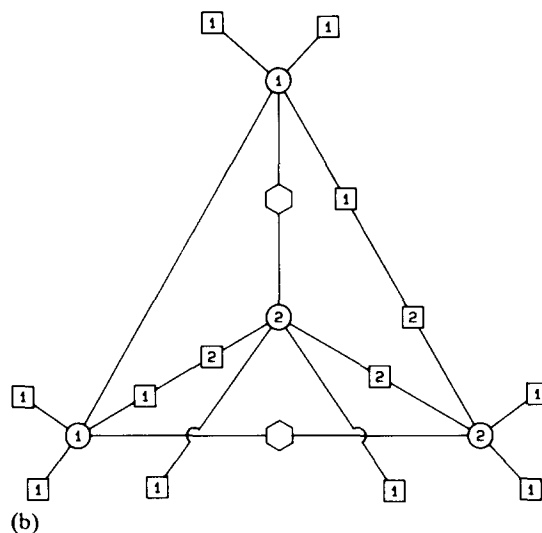
Four-circle diffraction data indicated an additional reflection condition  $h0l$  with  $l=2n$  only. This suggests  $Cc$  (no. 9 IT, non-centrosymmetric) and  $C2/c$  (no. 15 IT, centrosymmetric) as possible space groups. Structure refinement confirmed the centrosymmetric group.

### 3. Structural determination

Interpretation of the Patterson map (SHELXS-86 [13]) indicated the position of Ir. Further parameters of K, O and Li were obtained gradually from difference maps of previous refinements (SHELX-76 [14]). Finally, the refinement of all the parameters, including "anisotropic" thermal parameters for all the atoms, gave  $R = 0.0351$  and  $R_w = 0.0378$ , using 949 reflections with  $F_o > 3\sigma(F_o)$ .



(a)



(b)

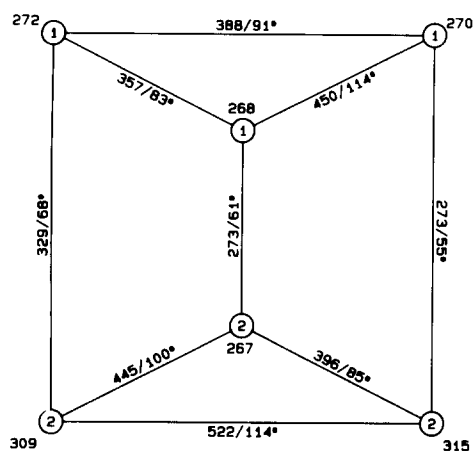
Fig. 2. (a) Schlegel projection and (b) Schlegel diagram of CP(Li) in  $K_3\{\text{Li}[\text{IrO}_4]\}$ :  $\square$ , K;  $\circ$ , O;  $\Delta$ , Ir.

For positional and "anisotropic" thermal parameters, see Table 2.

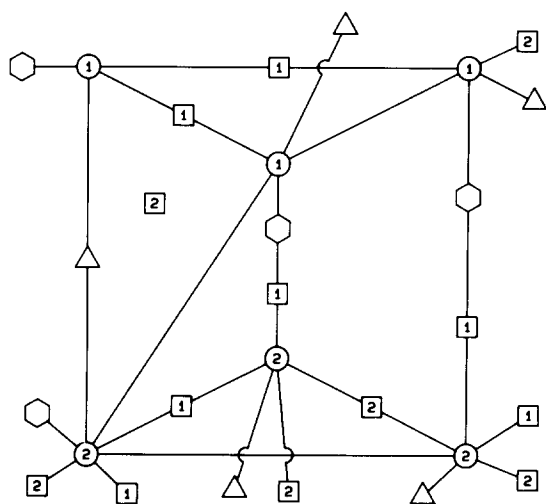
### 4. Structural description

According to  $K(1)_4K(2)_2Li_2Ir_2O(1)_4O(2)_4$ , the new iridate  $K_3\{\text{Li}[\text{IrO}_4]\}$  crystallizes with the twofold of gross composition in a new type of structure. Characteristic are Vierer single chains  $\infty[(O_{2/2}LiO_2IrO_{2/2})_2]$  "separated" from each other, which are arranged in accordance with the configuration of a densest packing of "tree-trunks". The square planar groups  $[\text{IrO}_4]^{4-}$  in these chains are almost vertical to each other; the dihedral angle is  $84.2^\circ$ . Table 3 gives the motifs of mutual adjunction, effective coordination numbers (ECoN) and mean fictive ionic radii (MeFIR) [15], as well as the coordinative distances.

This arrangement is similar to that which Hofmann and Hoppe found with  $K_3\{\text{Li}[\text{SiO}_4]\}$ . Admittedly there,



(a)



(b)

Fig. 3. (a) Schlegel projection and (b) Schlegel diagram of CP[K(1)] in  $K_3\{Li[IrO_4]\}$ :  $\Delta$ , Li;  $\square$ , K;  $\circ$ , O;  $\circ$ , Ir.

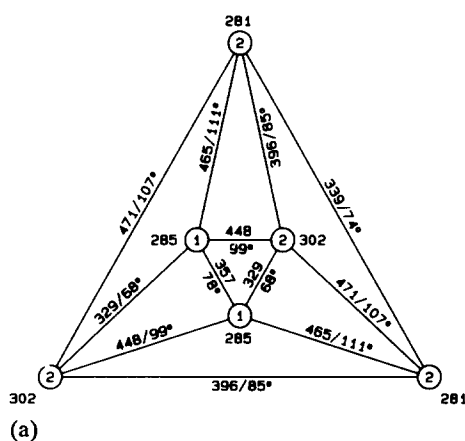
the chains  $\{LiSiO_4\}$  are based on edge-sharing tetrahedra of the coordination polyhedra (CP) of Si and Li.

#### 4.1. Primary structure

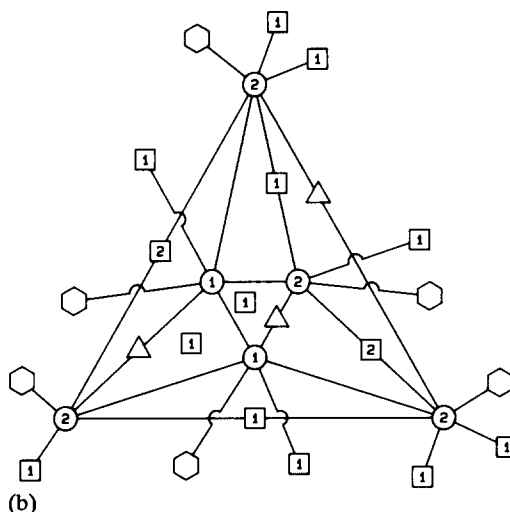
Two oxygen atoms of each crystallographic sort form an almost regular square around Ir (see Fig. 1). The distances  $d(\text{Ir}-\text{O})$  are 190.6 pm and 191.7 pm respectively; however, the shorter distances are those with O(1). The mean distance is 191.2 pm, which agrees excellently with that for all oxoiridates(IV) with square planar groups  $[\text{IrO}_4]^{4-}$  (191.1 pm [16]) known to date.

Li also has a coordination number (CN) of 4. The CP corresponds to a bisphenoid which is build with 2 O(1) and 2 O(2) (see Fig. 2(a)).

Both different crystallographic types of potassium have CN=6. There are 3 O(1) and 3 O(2) surrounding K(1) like a distorted trigonal prism. However, only oxygen atoms of the same crystallographic sort form the bases of CP[K(1)] (see Fig. 3(a)). In comparison,



(a)



(b)

Fig. 4. (a) Schlegel projection and (b) Schlegel diagram of CP[K(2)] in  $K_3\{Li[IrO_4]\}$ :  $\Delta$ , Li;  $\square$ , K;  $\circ$ , O;  $\circ$ , Ir.

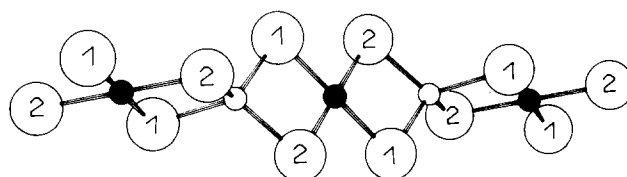


Fig. 5. Part of the Vierer single chain  $\frac{1}{2}[(\text{O}_{22}\text{LiO}_2\text{IrO}_{2/2})_2]$  for  $K_3\{Li[IrO_4]\}$  in detail: large numbered circles, O; small shaded circles, Ir; small open circles, Li;  $d(\text{Ir}-\text{O}(1))=190.6$  pm,  $d(\text{Ir}-\text{O}(2))=191.7$  pm,  $d(\text{Li}-\text{O}(1))=189.6$  pm,  $d(\text{Li}-\text{O}(2))=194.0$  pm,  $d(\text{Ir}-\text{Li})=272.3$  pm.

CP[K(2)] gives a distorted octahedron with a corrugated "waist". Here, 4 O(2) and 2 O(1) form the CP (see Fig. 4(a)).

#### 4.2. Secondary and tertiary structure

The CP(Ir) are isolated from one another, as are the CP(Li) (compare Figs. 1 and 2(b)). In comparison the CP[K(1)] are connected with each other via five edges and two corners, forming a complicated spatial network. The CP[K(2)] form corrugated chains along

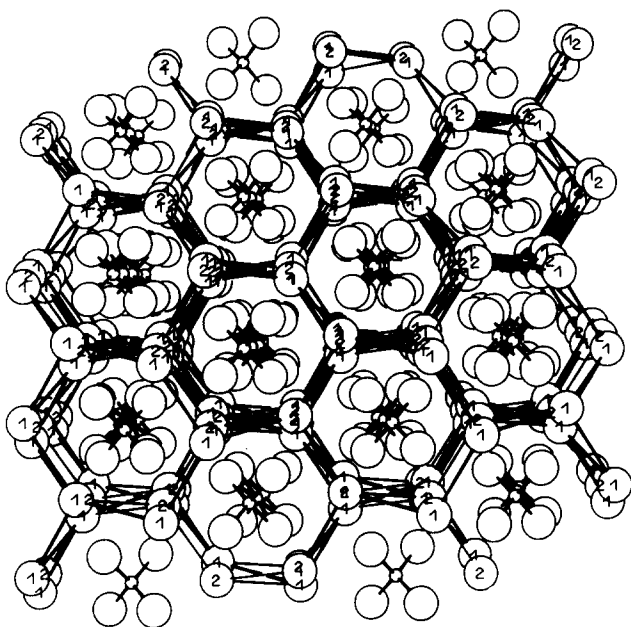


Fig. 6. Perspective view of the crystal structure of  $K_3\{Li[IrO_4]\}$ , emphasizing the “honey-comb-like” arrangement of K; large numbered circles, K; large open circles, O; small circles, Ir and Li.

TABLE 4. MAPLE for  $K_3\{Li[IrO_4]\}$  (in kilocalories per mole)

	MAPLE <sub>quaternary</sub>	MAPLE <sub>binary</sub>	*MAPLE	*MAPLE
1Ir <sup>4+</sup>	1827.4	2050.4	114.2	216.5
1Li <sup>+</sup>	196.8	146.2	196.8	373.1
2K(1) <sup>+</sup>	113.3	104.9	113.3	302.9
1K(2) <sup>+</sup>	116.0	104.9	116.0	326.5
2O(1) <sup>2-</sup>	507.2	585.5 <sup>a</sup>	126.8	240.4
2O(2) <sup>2-</sup>	508.5	$\left\{ \begin{array}{l} 1.5 \times 390.1^b \\ 0.5 \times 543.5^c \end{array} \right\}$	127.9	243.7
$\Sigma$	4398	4540	$\Delta = -141.6 = -3.12\%$	
$\Sigma'$		4413	$\Delta' = -14.4 = -0.33\%$	

$$\Delta = \Sigma \text{MAPLE}_{\text{quaternary}} - \Sigma \text{MAPLE}_{\text{binary}}$$

$$\Delta' = \Sigma \text{MAPLE}_{\text{quaternary}} - \Sigma' \text{MAPLE}_{\text{binary}}$$

$$*\text{MAPLE} = \text{MAPLE}/q^2.$$

$$*_i \text{MAPLE} = *\text{MAPLE } d_k.$$

<sup>a</sup>From IrO<sub>2</sub>.

<sup>b</sup>From K<sub>2</sub>O.

<sup>c</sup>From Li<sub>2</sub>O.

[001] at  $y \cong 0$  and  $y \cong 1/2$ , by sharing trans-edges (O(2)–O(2)).

It should be noted that, as we expected, the CP(Ir) and CP(Li) are linked via trans-edges to Vierer single chains  $\frac{1}{2}[(O_{2/2}LiO_2IrO_{2/2})_2]$ . These run parallel to [101], alternating at  $y \cong 1/4$  and  $y \cong 3/4$ , respectively, and are “separated” from each other. The square planar groups  $[IrO_4]^{4-}$  of every chain are oriented nearly vertically to each other; the dihedral angle is 84.2°. The Vierer single chains are arranged according to the configuration of a densest packing of “tree-trunks”. Figure 5 shows

TABLE 5. CHARDINO charge distribution for  $K_3\{Li[IrO_4]\}$

	2O(1)	2O(2)	$\Sigma(\text{cation})$
1Ir	+1.923 –0.962	+2.087 –1.038	+4.01
1Li	+0.505 –0.254	+0.494 –0.246	+1.00
2K(1)	+0.613 –0.623	+0.373 –0.377	+0.99
1K(2)	+0.346 –0.171	+0.673 –0.329	+1.02
$\Sigma Q(O)$	–2.01	–1.99	

Charge distributions are given as, for example, +1.923 [Ir–O(1)] and –0.962 [O(1)–Ir], and the sums  $\Sigma(\text{cation})$  and  $\Sigma(O)$ .

part of such a chain in detail.

The crystal structure of  $K_3\{Li[IrO_4]\}$  is quite markedly characterized by the arrangement of these Vierer single chains. In addition, the mean distances  $\bar{d}(\text{Li–O}) = 191.8$  pm and  $\bar{d}(\text{Ir–O}) = 191.7$  pm correspond nearly exactly. This is why the term “lithooxoiridate(IV)” is necessary to emphasize these very structural peculiarities.

Each K atom connects three different chains via edges of CP(Ir) or CP(Li). The view along [101] indicates that all the K atoms are arranged according to a honeycomb-like network with hexagonal cross-section. The “walls” of these honeycombs separate the Vierer single chains running within the hexagonal cavities (see Fig. 6).

## 5. Madelung part of the lattice energy

Table 4 gives the Madelung part of the lattice energy (MAPLE) [17] for  $(K_3\{Li[IrO_4]\})$  and compares individual contributions of the ions with the values for binary oxides. As usual for oxoironates(IV), we find that  $\Sigma \text{MAPLE}_{\text{binary}}$  is considerably greater than the value for the polynary oxide. A reason for this might be that, for IrO<sub>2</sub>, there is still no structure refinement based on single-crystal data available.

By subtraction of the MAPLE for the alkaline or earth-alkaline oxides from the MAPLE for polynary oxoironates(IV), one obtains MAPLE(“IrO<sub>2</sub>”); e.g. for  $K_3\{Li[IrO_4]\}$ ,  $\text{MAPLE}(\text{“IrO}_2\text{”}) = \text{MAPLE}(K_3\{Li[IrO_4]\}) - 1.5 \text{MAPLE}(K_2O) - 0.5 \text{MAPLE}(Li_2O)$ . The mean value  $\overline{\text{MAPLE}(\text{“IrO}_2\text{”})}$  of all single-crystal data-refined oxoironates(IV) to date is 3093 kcal mol<sup>–1</sup> (cf. ref. 4). From  $\text{MAPLE}(\text{“IrO}_2\text{”}) + 1.5 \text{MAPLE}(K_2O) + 0.5 \text{MAPLE}(Li_2O)$  we obtain  $\text{MAPLE}(K_3\{Li[IrO_4]\})_{\text{“binary”}} = 4413$  kcal mol<sup>–1</sup>, which fits well with the value for  $K_3\{Li[IrO_4]\}$ .

## 6. Charge distribution

Table 5 shows the charge distribution obtained via CHARDINO [18] for  $K_3\{\text{Li}[\text{IrO}_4]\}$ . The values for the cations as well as for the anions agree very well with the expected values.

## 7. Concluding remarks

The achievement of the synthesis of  $K_3\{\text{Li}[\text{IrO}_4]\}$  via an "exchange reaction" and its successful crystal structure determination opens the door to a wide field of possible new oxoiridates(IV) containing Li. The first question, of course, concerns the possible existence of additional members of the series  $A_{4-n}\text{Li}[\text{IrO}_4]$ , such as  $\text{Na}_3\text{Li}[\text{IrO}_4]$  and  $\text{Cs}_3\text{Li}[\text{IrO}_4]$ .

What about oxides such as  $\text{K}_2\text{Li}_2[\text{IrO}_4]$  or even  $\text{CsLi}_3[\text{IrO}_4]$ ? We believe that the side view on silicates might be a helpful guide in trying to prepare new lithooxoiridates. Some oxides rich in Li are known to have unique crystal structures; e.g.  $\text{RbLi}_5\{\text{Li}[\text{SiO}_4]\}_2$  [19] as well as  $\text{CsKNa}_2\text{Li}_8\{\text{Li}[\text{SiO}_4]\}_4$  [20]. Synthesis of oxoiridates(IV) such as  $\text{RbLi}_5\{\text{Li}[\text{IrO}_4]\}_2$  or  $\text{CsKNa}_2\text{Li}_8\{\text{Li}[\text{IrO}_4]\}_4$  might be fruitful steps on the way to preparing still unknown  $\text{Li}_4\text{IrO}_4$ .

## Acknowledgments

The collection of X-ray intensities was carried out by Dr. M. Serafin. The calculations on the structure refinements were performed on a Control Data Cyber 860 system of the Hochschulrechenzentrum of the Justus-Liebig-Universität Giessen. We would like to thank

the Fonds der Chemischen Industrie and the Deutsche Forschungsgemeinschaft for their kind financial support.

## References

- 1 G. Meyer, *Thesis*, Giessen, 1976.
- 2 J. Kissel and R. Hoppe, *Z. anorg. allg. Chem.*, 570 (1989) 109.
- 3 D. Fischer and R. Hoppe, *Z. anorg. allg. Chem.*, 586 (1990) 106.
- 4 K. Mader and R. Hoppe, *Z. anorg. allg. Chem.*, 619 (1993) 1647.
- 5 P. Kroeschell and R. Hoppe, *Naturwissenschaften*, 73 (1985) 327.
- 6 P. Kroeschell, *Thesis*, Giessen, 1986.
- 7 K. Mader and R. Hoppe, *Z. anorg. allg. Chem.*, 614 (1992) 30.
- 8 R. Hofmann and R. Hoppe, *Z. anorg. allg. Chem.*, 560 (1988) 35.
- 9 W. Klemm and K. Wahl, *Z. anorg. allg. Chem.*, 283 (1956) 196.
- 10 W. Klemm and H. Scharf, *Z. anorg. allg. Chem.*, 303 (1960) 263.
- 11 R. Hoppe, *J. Solid State Chem.*, 64 (1986) 372.
- 12 A. Simon, *J. Appl. Crystallogr.*, 3 (1970) 11.
- 13 G. Sheldrick, SHELX-76, program for crystal structure determination, Cambridge, 1976.
- 14 G. Sheldrick, SHELX-76, Programm zur Lösung von Kristallstrukturen, Göttingen, 1986.
- 15 R. Hoppe, *Z. Kristallogr.*, 150 (1979) 23.  
G. Meyer and R. Hoppe, *Z. anorg. allg. Chem.*, 420 (1976) 40.
- 16 K. Mader, *Thesis*, Giessen, 1993.
- 17 R. Hoppe, *Z. anorg. allg. Chem.*, 283 (1956) 196; *Angew. Chem.*, 78 (1966) 52; *Angew. Chem. Int. Ed. Engl.*, 5 (1966) 95; *Angew. Chem.*, 82 (1970) 25; *Angew. Chem. Int. Ed. Engl.*, 9 (1970) 25; *Adv. Fluorine Chem.*, 6 (1970) 387.
- 18 R. Hoppe, to be published.
- 19 K. Bernet and R. Hoppe, *Z. anorg. allg. Chem.*, 592 (1991) 93.
- 20 J. Hofmann, R. Brandes and R. Hoppe, *Z. anorg. allg. Chem.*, in press.